Environmental Science
Water Research & Technology

ROYAL SOCIETY OF CHEMISTRY

PAPER

View Article Online
View Journal | View Issue

Cite this: *Environ. Sci.: Water Res. Technol.*, 2026, **12**, 1116

Towards scalable electrochemical reduction cells for hexavalent chromium

Collin A. Dunn, Alan Rassoolkhani, Cameron Lippert and James Landon *

Received 26th August 2025,
Accepted 8th January 2026

DOI: 10.1039/d5ew00828j

rsc.li/es-water

The ability of electrochemical cells with carbon-based anodes and cathodes to reduce hexavalent chromium (Cr(VI)) to trivalent chromium (Cr(III)) was investigated over a range of applied potentials and feed pH values. These cells reduced >99% of the 200 ppm Cr(VI) present with a residence time below one minute when applying at least 0.75 V to solutions with a pH below 2.5. Loss of reduction at higher pH values is associated with the predicted formation of solid chromium compounds on the cathode surface due to local pH shifts during operation. A long-term breakthrough study was performed comparing the all-carbon cell to one with a mixed-metal oxide (MMO) anode. Near total reduction of Cr(VI) to Cr(III) was maintained by the carbon cell for 4 hours of operation at 1.5 V before higher effluent Cr(VI) concentrations were seen. While the MMO cell did not suffer a reduction in performance, cost savings with carbon electrodes *versus* MMO could be quite substantial. Postmortem analysis of the carbon anodes shows increased resistivity, which correlates to the loss of reductive capacity. Based on these results, commercial projections were possible, which show that this type of electrochemical cell may be an environmentally and economically sound alternative to sulfite addition when managing process streams containing hexavalent chromium.

Water impact

Hexavalent chromium (Cr(VI)) is a waterborne toxin with severe impacts to both human life and the environment at large. The treatment approach presented in this work nearly completely reduces the pollutant to the less toxic trivalent chromium (Cr(III)) using only low voltage electricity. The proposed treatment approach also works to reduce water pollution and water use by obviating the need to manufacture and deploy chemical additives for Cr(VI) treatment. By making it simpler and cheaper to treat for Cr(VI), this work seeks to empower both municipalities and generators with additional tools for mitigating the effects of this toxin.

Introduction

The harmful effects of hexavalent chromium (Cr(VI)) have been extensively studied, which has led to a sharp curtailing of its use in recent decades.[1–3] However, in certain industries, such as steel manufacturing and electropolishing, Cr(VI) is still quite pervasive due to its favorable properties and preferred processing methods.[3] Therefore, treatment and removal of Cr(VI) from various wastewater effluents remains a necessity. Federal, state, and local municipalities typically set industrial discharge requirements for total chromium to <3 ppm and hexavalent chromium to <1 ppm to achieve low levels of chromium in drinking water supplies.[4]

In many commercial applications, Cr(VI) is chemically reduced in wastewater streams through the use of sodium metabisulfite (SMBS), or similar analogs.[5,6] While effective, the process can be poorly controlled, relying on oxidation–reduction potential (ORP) probes to determine when Cr(VI) has been fully reduced. In addition, process upsets can lead to inadequate addition of SMBS, resulting in waste treatment needing to be repeated and halting production processes. Chemical storage and the associated dust from SMBS must also be tracked and controlled to avoid equipment downtime and safety incidents. Most important, transport of SMBS to waste processing facilities involves shipping/receiving logistics, and possible supply disruptions, leading to vulnerabilities at the site. Alternative treatment methods exist such as chemical coagulation, but they often suffer from similar complications to SMBS.[7] The possibility of using non-chemical methods of reduction (electrochemical processes) are therefore being sought where electricity is the input *versus* a chemical needing transport to the site.

Electrochemical methods offer distinct advantages over conventional chemical technologies for the reaction and abatement of concentrated metals in waste streams.[8–10] For metals such as Cr(VI), electrochemical cells can be built that target the reduction of this compound to Cr(III) (eqn (1)). The redox potential at 1.35 V *vs.* NHE gives a high degree of

ElectraMet, 749 W. Short St., Lexington, KY 40508, USA.
E-mail: james.landon@electramet.com

selectivity over other common metal contaminates such as iron and copper, commonly found in metal fabricating processes or electropolishing, which are far less noble, with redox potentials at 0.78 and 0.34 V *vs.* NHE, respectively. Additionally, any excess reaction of non-chrome species would galvanically react with untreated hexavalent chromium to indirectly give the desired reduced species. After reduction to trivalent chromium, which is a much more benign Cr species capable of being easily precipitated out of solution and recycled or transported to a waste site.

$$HCrO_4^- + 7H^+ + 3e^- \leftrightarrow Cr^{3+} + 4H_2O; \quad E^\circ = 1.35 \text{ } vs. \text{ NHE} \quad (1)$$

Beyond the selectivity offered by electrochemical processes, real-time feedback of the metals removal process is available through current generated on the electrode surfaces, resulting in potential systems-wide automation to better handle process disruptions and maintain discharge compliance. Finally, since these processes are run on electricity, supply chain difficulties are often lessened as system reliability can more directly follow electrical grid reliability.

In the construction of an electrochemical process for Cr(VI) reduction to Cr(III), a few key factors must be taken into account. First, effective reduction of Cr(VI) to single digit parts per million levels, or lower, must be achieved to reach most discharge compliance limits. Second, the process must be reliable, maintaining these effluent concentrations for days, weeks, months, and possibly years. Ultimately, the cost must be competitive with existing processes. While chemical addition of SMBS may have notable deficiencies, limited budgets are typically afforded to wastewater treatment processes, so materials must be chosen accordingly.

Electrochemical processes have been used in the past to accomplish reduction of Cr(VI) to Cr(III).[11–13] Rodriguez-Valadez *et al.* examined the use of reticulated vitreous carbon electrodes in a parallel plate reactor to reduce Cr(VI), examining the impact of reduction potential, pH, and flow rate, among other factors, on the reduction kinetics and efficiencies.[14] Separate anolyte and catholyte chambers were used in this reactor design. Roberts *et al.* evaluated the use of a porous carbon felt cathode in the reduction process in a flow-through electrochemical cell. The current density and pH were evaluated in this study on the reduction kinetics.[15] Stern *et al.* investigated the use of glassy carbon electrodes for the detection of Cr(VI) in a variety of water conditions.[16] Su *et al.* investigated redox-active electrodes for the removal and reduction of Cr(VI) to Cr(III).[17] While all of these systems demonstrated the capability for electrochemical Cr(VI) reduction and contributed to the experimental design landscape, reaction times could be long, nearly 60 min for full reduction of 100 ppm Cr(VI) in a 100 ml feed in the case of Rodriguez-Valadez *et al.* and even longer in the case of Roberts *et al.* Therefore, an electrochemical cell with near complete water recovery and high processing rate could advance these separations.

In this manuscript, a new electrochemical cell will be reviewed (Fig. 1), highlighting the capability for fast, continuous, and stable Cr(VI) reduction. Flow is directed through a porous graphitic carbon cathode while a dense activated carbon film or a mixed metal oxide (MMO) anode is used. At the cathode, Cr(VI), in the form of chromate, will be reduced to Cr(III) and water, while the anode will balance the reaction through either a combination of capacitive charging and carbon oxidation with the activated carbon film or water oxidation to oxygen gas using the more traditional MMO electrode. While the use of an activated carbon film anode has been shown before in capacitive deionization (CDI) and electrodialysis reversal (EDR), the combination of faradaic Cr(VI) reduction and capacitive charge storage with carbon electrodes is new in this work.[18,19] The effect of the anode electrode material will be evaluated both for performance as well as for cost. Projections towards future performance and lifetime gains will be evaluated.

Materials and methods

Chemical, cell, and analytical components

Deionized water was purchased from Superior Chemicals Inc. Chromium (VI) oxide was purchased from Sigma-Aldrich. 98 wt.% sulfuric acid was purchased from Superior Chemicals Inc. All reagents were used as purchased with no additional purification. Microporous capacitive activated carbon film anodes were obtained from LiCAP Technologies Inc. Activated carbon films had an areal density of approximately 32 mg cm^{-2} and specific surface areas of approximately 1100 m^2 g^{-1}. Cathodes were cut from graphitic carbon felt from SGL Carbon with uncompressed thicknesses of approximately 2.5 mm and specific surface areas of <5 m^2 g^{-1}. Grade 2 titanium current collectors were obtained from Augur Metal Products Inc. For experiments utilizing MMO anodes, titanium current collectors were coated by Optimum Anode Technologies with an iridium oxide coating. Characterizations for the electrode materials, including density, thickness, and other physical properties can be found in the supplemental information. A polyethylene-based separator was implemented between each anode and cathode pair for the separation experiments.

Cr(VI) concentrations were measured using a Hach DR 3900 colorimeter with Hach TNT 854 Cr(VI)/total chromium tests. Potential was applied to the cell by a GW Instek GPS-4303 laboratory DC power supply. Potential and current profiles of the electrochemical cell were recorded *via* a Graphtec 220 digital recorder. A Cole-Parmer Master Flex L/S peristaltic pump equipped with a 316 stainless steel rotor and platinized silicone pump tubing was used for fluid pumping.

Electrochemical characterization

Electrochemical activity for each electrode type was characterized in a sulfuric acid solution pH adjusted to 1.5. Carbon electrode characterizations were further carried out in 200 ppm Cr(VI) solution, made using chromium(VI) oxide.

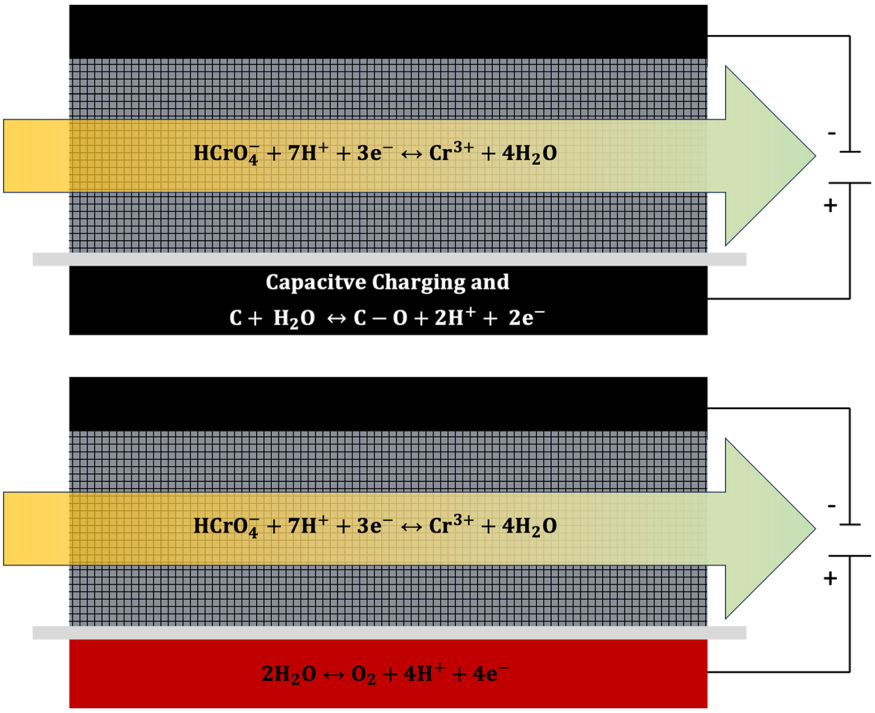

Fig. 1 Schematic of electrochemical Cr(VI) reduction cells using carbon anodes (top) and MMO anodes (bottom).

Measurements were made using a 3-electrode configuration with the activated carbon film, graphitic carbon felt, or MMO serving as the working electrode, platinized titanium as the counter electrode, and Ag/AgCl as the reference electrode. An exposed surface of approximately 1 cm^2 was used for the characterization studies with electrical contact being made using a titanium current collector or graphite block. For the anodic reaction, linear sweep voltammograms (LSV) were carried out at a rate of 10 mV s^{-1} up to 1.6 V *vs.* Ag/AgCl. The onset potential for Cr(VI) reduction was identified using the same setup utilizing graphitic carbon felt as the working electrode. For the cathodic reaction, LSVs were carried out at a scan rate of 10 mV s^{-1} from 0.8 to −0.4 V *vs.* Ag/AgCl.

Cell assembly

The electrochemical cells employed in this study consist of a high-density polyethylene (HDPE) base plate, a silicone rubber gasket, 3 pairs of cathodes and anodes electrically isolated by a polyethylene-based separator, and a second silicone rubber gasket. Electrical connections to the current collectors are made with threaded titanium rods. Small gasketed washers were used to prevent leaks. Standoffs of sufficient total length to nearly cover the exposed rods are implemented, and nuts are tightened on the threaded ends of the rods so that the cell is compressed. The stack-cap assembly is then attached to a cell body and a bottom cap (with a central threaded port) using a pair of O-rings and worm-drive clamps. Finally, acid-resistant, female push-to-connect fittings are screwed into the top and bottom caps. The result is a water-tight assembly where all components exposed to the process water are resistant to corrosion, and potential may be applied by simply attaching leads to the exposed rods on the top of the cell. A picture of the electrochemical cell used in these studies is found in the supplemental information in Fig. S23.

Feed preparation

All feed solutions used in this study contained 200 ppm Cr(VI). For each separation, a desired amount of solution was chosen, and that volume of water was measured and poured into a 1-gallon HDPE container. This water was then acidified to the desired pH by the addition of 18 M sulfuric acid, added dropwise by a transfer pipette. Once the target pH was reached, the required mass of CrO_3 was added to a tared weigh boat on an analytical balance and stirred into the container of acidified water. A nearly instant color change from colorless to orange was observed, as was the total dissolution of the solid CrO_3.

Cr(VI) removal at varied pH/potential

The ability of cells with carbon-based anodes to reduce hexavalent chromium was investigated by two sets of experiments. The experimental set up is outlined in Fig. 2. Firstly, separation performance was measured at a constant feed pH of 1.0 at various applied potentials ranging from 0.5 V to 1.5 V. Secondly, a potential of 1.5 V was applied for the treatment of various feed streams with pH values ranging from 1 to 4. For both sets of experiments, a flow rate of 12 mL min^{-1} was chosen, resulting in a residence time of 55 seconds. Water was pumped into the bottom of the cell body

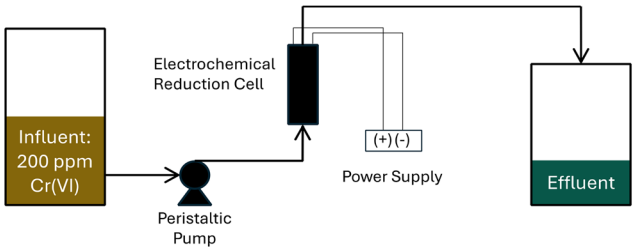

Fig. 2 Experimental setup of the electrochemical reduction cell.

and exited from the top, demonstrating reduction of Cr(VI) in a single pass through a cell containing just one inlet and one outlet. For each experiment, a completely new cell was assembled to ensure that there were no aging effects or residual chromium species present at the start of an experiment. One set of anode/cathode rods were used to attach leads for directly reading the applied potential. Another set of rods were used to deliver power to the cell. These leads were routed through a digital potential logger, allowing the current profile to be recorded.

At the start of an experiment, the pump is switched on. Once water begins to flow out of the cell into the effluent collection container, data collection for the current is started, and the power supply is switched on and set to the appropriate potential. After 15 minutes of operation, current logging is stopped, and a sample is taken directly from the outlet of the cell and analyzed for Cr(VI) content with colorimetry tests.

The charge efficiency was also calculated for each separation using eqn (2) shown below.

$$\text{Charge Efficiency} = \frac{\frac{\Delta[\text{Cr(VI)}]\times V}{\text{MW}_{\text{Cr}}}\times F\times n}{Q} \quad (2)$$

where Δ[Cr(VI)] is the concentration change from influent to effluent in g L^{-1}, V is the volume in L of solution treated (flow rate over time), MW_{Cr} is the molecular weight of Cr in g mol^{-1}, F is Faraday's constant (96 485 C mol^{-1}), n is the number of electrons to reduce Cr(VI) (3), and Q is the charged passed during treatment in C.

Long-term Cr(VI) removal

Long-term Cr(VI) reduction performance of the carbon-based anodes was compared to that of MMO-based anodes by continuously feeding both types of cells a 200 ppm Cr(VI) stream at pH 1.5 to reduce and regularly sampling the effluent until a "breakthrough" of Cr(VI) is detected. In the interest of possibly capturing an early breakthrough, liquid sampling is spaced closely at the beginning of the experiments but becomes less frequent with time.

Results and discussion

The activated carbon film and graphitic carbon felt as well as MMO electrode materials were first evaluated for their activity in pH 1.5 sulfuric acid electrolyte. In the case of the graphitic carbon felt and activated carbon film, 200 ppm Cr(VI) was also added to the solution using chromium(VI) oxide. For the given process stream, the redox potential to achieve 200 ppm Cr(VI) reduction to 0.2 ppm is 1.29 V *vs.* NHE at pH 0 (eqn (3)), forming Cr(III) in the process.

$$E = 1.35 + 0.0197\log\frac{\text{Cr}^{6+}}{\text{Cr}^{3+}} - 0.137\ \text{pH} \quad (3)$$

The reactions at the anode will vary based on the electrode used in the study. The reaction at the activated carbon film anode could take place as either capacitive adsorption over a range of operating potentials or through carbon oxidation (eqn (4)).[20]

$$\text{C} + 2\text{H}_2\text{O} \leftrightarrow \text{CO}_2 + 4\text{H}^+ + 4\text{e}^-;\quad E^\circ = 0.207\ \text{V } \textit{vs.}\ \text{NHE} \quad (4)$$

This equation represents carbon oxidation to carbon dioxide, but other surface carbon oxides and hydroxides can form, which have been noted in capacitive deionization literature.[21–24] Potential steps were used during separation studies to first define proper operating conditions for the all-carbon cell. For experiments utilizing the MMO anode, the reaction will be water oxidation to oxygen gas (eqn (5)).

$$2\text{H}_2\text{O} \leftrightarrow \text{O}_2 + 4\text{e}^- + 4\text{H}^+;\quad E^\circ = 1.23\ \text{V } \textit{vs.}\ \text{NHE} \quad (5)$$

The onset potential is seen in the linear sweep voltammogram (LSV) for each electrode, which can be seen in Fig. 3. For the graphitic carbon felt, current onset is observed at 0.8 V *vs.* NHE with a maximum at 0.6 V *vs.* NHE. While far more cathodic than the theoretical potential, reduction still takes place at a much more positive potential than hydrogen evolution at pH 1.5 (−0.09 V *vs.* NHE). To confirm that the reduction peak seen in this LSV is due to

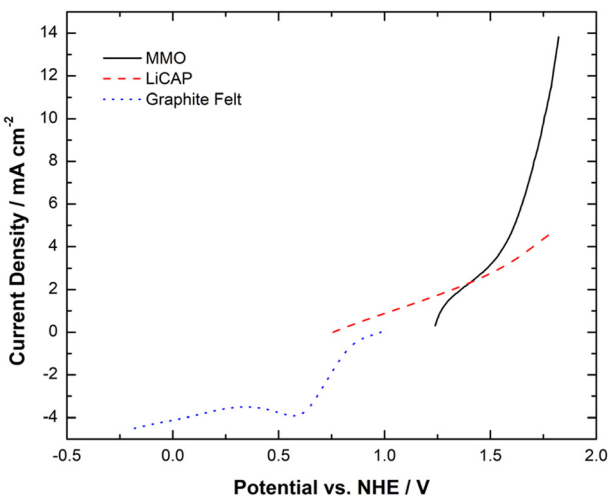

Fig. 3 LSV at 10 mV s^{-1} in 200 ppm Cr(VI) in pH 1.5 sulfuric acid for MMO (black line), activated carbon film (red dash), and graphitic carbon felt (blue dot). Cr(VI) was not present for water oxidation studies using the MMO electrode.

Cr(VI) reduction and not a redox active surface group, LSVs were conducted with and without 200 ppm Cr(VI) being present (Fig. S1). No reduction peak is seen without the presence of Cr(VI). For the activated carbon film anode, the onset potential was generally observed at 0.8 V *vs.* NHE. When paired with the onset potential for Cr(VI) reduction, the reaction is near spontaneous, although approximately 0.5 V of overpotential would be needed to reach the maximum reaction rates. For the MMO electrode, the onset potential is seen at 1.5 V. While the MMO is an excellent oxidation catalyst, the 4-electron oxygen evolution reaction coupled with the higher thermodynamic potential will require a higher overall potential compared to the activated carbon film anode. It should be noted that while higher current density may be available with the LiCAP carbon film anode at lower voltages, accessible charge will be finite once capacitive sites are filled and easily accessible surface groups are oxidized. All potentials are referenced to reversible hydrogen electrode [V_{NHE}; $V_{NHE} = V_{Ag/AgCl} + 0.197\ V + 0.059\ pH$].

Beyond characterizations through LSVs, a Pourbaix diagram was also constructed using equilibrium equations for chromium and water at potentials ranging from 0.2–1.4 V and pH ranging from 0–7. Shown in Fig. 4 are the resulting equilibrium states (black lines) for 200 ppm chromium in a chromium–water system using equations provided in the Atlas of Electrochemical Equilibria in Aqueous Solutions.[25] Oxygen evolution (red dashed line) is shown as well. While industrial streams can be more complex than the Pourbaix diagram being shown here, it is a useful thermodynamic guide when assessing these systems. Voltages higher than the oxygen evolution potential will be needed to drive reactions at an MMO anode, which is a pH-dependent reaction. Voltages below the Cr(VI) line will be needed to drive reactions at the graphitic carbon felt cathode to form Cr(III), also a pH-dependent reaction. At low enough pH values, less than 1, these reactions would appear to be spontaneous. However, due to the overpotentials needed at both electrode surfaces, as mentioned above for the LSVs, cell voltages of >0.5 V are needed in reality. Similar Pourbaix diagrams have been developed by others in evaluating electrochemical Cr(VI) reduction processes.[17] Importantly in this diagram is the presence of $Cr(OH)_3$, which can form at pH values as low as 4.7. Given that this species can result in solids precipitating at the cathode surface, its avoidance is critical to developing a stable Cr(VI) reduction process. Therefore, the first separations evaluated the impact of applied potential and operating pH on Cr(VI) reduction.

Effect of applied potential on reduction of Cr(VI)

A series of experiments were conducted using electrochemical cells with carbon-based anodes to reduce hexavalent chromium in a pH 1 feed containing 200 ppm Cr(VI). A flow rate of 12 ml min^{-1} was used as a benchmark for all separation studies as it allowed for a residence time of <1 min. Additional residence time could be used to ensure Cr(VI) reduction, but it would have less commercial relevance as system sizes to treat defined flow rates and concentrations would grow with higher residence times. An acidic feed was chosen to prevent the formation of insoluble reduction products inside the cell and maximize removal efficiency. While hexavalent chromium readily dissolves in water over a wide pH range, Cr(II) and Cr(III) salts can form insoluble deposits at less acidic pH values, potentially blocking flow and access to reaction sites on the cathode. As can be seen in Fig. 5, increased potential decreases the concentration of Cr(VI) in the effluent with 98% conversion achieved at 0.5 V and a maximum conversion of 99.97% achieved by 1.25 V. The 98.1% reduction of Cr(VI) seen at 0.5 V is a testament to the relative thermodynamic ease of this reaction. Further reductions in this work were carried out at 1.5 V as maximum conversion efficiency (0.07 ppm effluent) was achieved at that operating condition with no loss of charge efficiency.

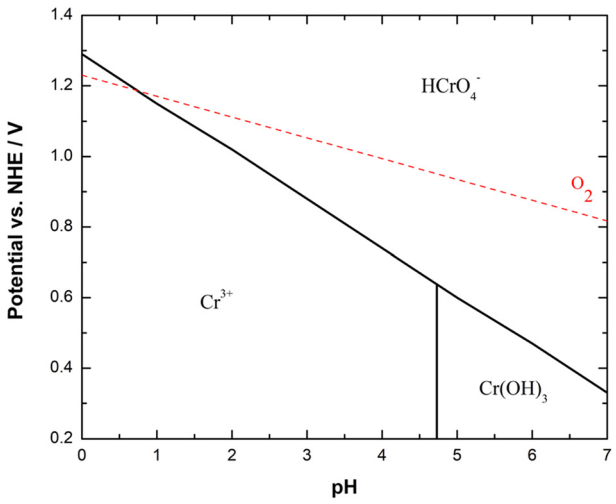

Fig. 4 Pourbaix diagram generated from equations in Atlas of Electrochemical Equilibria in Aqueous Solutions for 200 ppm Cr.[25]

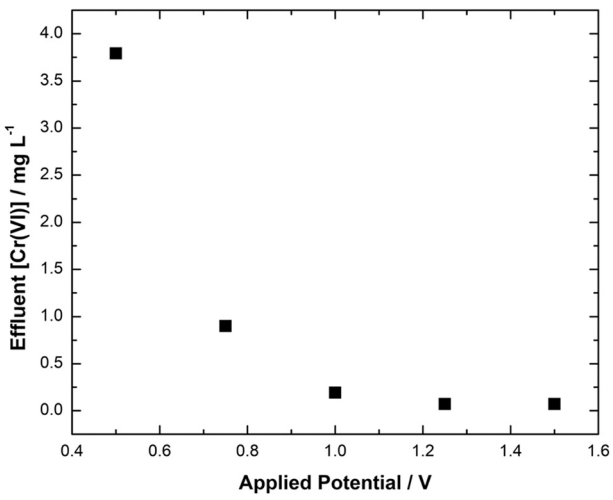

Fig. 5 Effluent Cr(VI) concentration *vs.* applied potential at feed pH 1 for 200 ppm Cr(VI) feed solution at a flow rate of 12 ml min^{-1}.

Effect of solution pH on reduction of Cr(VI)

Based on eqn (1), the rate of Cr(VI) reduction is dependent on system pH, and acidic environments would increase the conversion rates. Industrial streams will often have variation in their waste stream compositions. To determine the robustness of this separation technique, performance was compared at varying pH values while maintaining a given Cr(VI) influent concentration and a 1.5 V applied potential.

For 200 ppm Cr(VI) feeds, over 99.9% of the Cr(VI) is reduced when operating at a pH of 1, 1.5, or 2 (Fig. 6). However, upon increasing the feed pH to 2.5, only 86.5% of the Cr(VI) is reduced. This trend continues with increasing feed pH, with nearly half of the Cr(VI) remaining at a pH of 4. This is supported by the current transient, where the total charge passed over the duration of the experiment with the pH 1 feed was 165 C compared to 74 C at pH 4 (Fig. S2). Additionally, current measurements taken at the 10 minute mark decrease with increasing pH, starting at pH 2.5 (Fig. S3–S7).

Another explanation of this loss of separation is due to the accumulation of solids on the graphitic carbon felt cathode, which is supported by the appearance of the cathodes after the cells were disassembled post-separation. Images of the cathodes (Fig. S8–S12) show that at feed pH values of 2.5, 3, and 4 there are discolorations visible that appear to mirror the areas in most intimate contact with the current collectors. While a Pourbaix diagram would imply that there should be no issue reducing Cr(VI) from a feed stream with a pH of 3, in practice the local pH shift upwards at the cathode could be far more extreme resulting in the precipitation of chromium species. These results imply that the deposits are accumulating first in the areas of lowest electrical resistance. No such discolorations are seen with the cathodes used in the pH 1.5 experiment, and only slight discolorations are present with the pH 2 experiment. It should also be noted that while these experiments show the impact of feed pH on the depth of Cr(VI) reduction for a 200 ppm Cr(VI) influent, higher influent concentrations would have an even larger impact on the local pH change at the cathode due to the added proton consumption during the reduction process (eqn (1)), further limiting Cr(VI) reduction. Taking these results together with the results of the variable potential experiments, an electrochemical system for the reduction of 200 ppm Cr(VI) would preferably be operated at a potential of 1.5 V and at a feed pH of no more than 2.0.

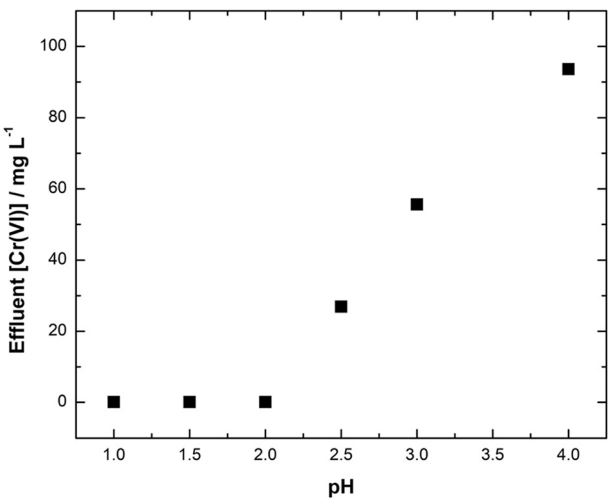

Fig. 6 Effluent Cr(VI) concentration *vs.* feed pH at 1.5 V of applied potential for 200 ppm Cr(VI) feed solution at a flow rate of 12 ml min^{-1}.

Long term Cr(VI) removal studies

The prior studies were conducted on electrochemical cells that operated for less than 30 minutes before being switched off and deconstructed. For lifetime tests, the cell was operated with a 200 ppm Cr(VI) feed at 1.5 V continually until breakthrough of untreated Cr(VI) occurred. The lengthier cycles used in this portion of the study exceeded the typical charging time periods used in CDI studies meaning that Cr(VI) reduction would transition from being balanced by capacitive charge storage and would instead be balanced by carbon oxidation. The feed was adjusted to pH 1.5, since there was no discoloration or solid accumulation previously seen on the electrode surface with this pH. Any decrease in performance could then be attributed to a loss of activity of the carbon as opposed to material coverage. It is typical for carbon electrodes to be attrited in use, both by chemical (carbon oxidation) and mechanical (delamination and friability) wear. To determine if performance decreases were a result of a change to the anode or cathode, the experiment was repeated with MMO-coated titanium anodes due to their exceptional stability in aggressive media and a functional lifetime measured in years.[26]

As can be seen in Fig. 7, the all-carbon cell maintained an effluent Cr(VI) concentration of <0.1 ppm until 4 hours had elapsed, at which point the effluent contained 2.2 ppm Cr(VI). Additional samples taken at 5 and 6 hours show a consistent effluent concentration of approximately 15 ppm Cr(VI). The companion cell made with an MMO-based anode was the more consistent and effective of the pair, maintaining reduction of Cr(VI) down to the effective LOD of the testing method for all 6 hours of testing (Fig. 8). Over the course of 6 hours of operation, each of these experiments processed a total of over 4.3 L of feed solution. Pictures of the product effluents can be found in Fig. S13 and S14. The degradation in performance seen with the all-carbon cell can be attributed to the filling of capacitive adsorption sites and oxidation of the anode steadily increasing electrode resistance. Oxidation is a common occurrence for carbon electrodes and supports, and if more capacitive sites were available, longer run times and more limited oxidation may be possible.[27,28] However, given the cost differential between the two anode materials (*e.g.* ~$10 per m^2 *vs.* ~$3000 per m^2), if their lifetime can be extended and their mode of failure can be better anticipated, they may become a promising material choice for this and other electrochemical-based removal processes.

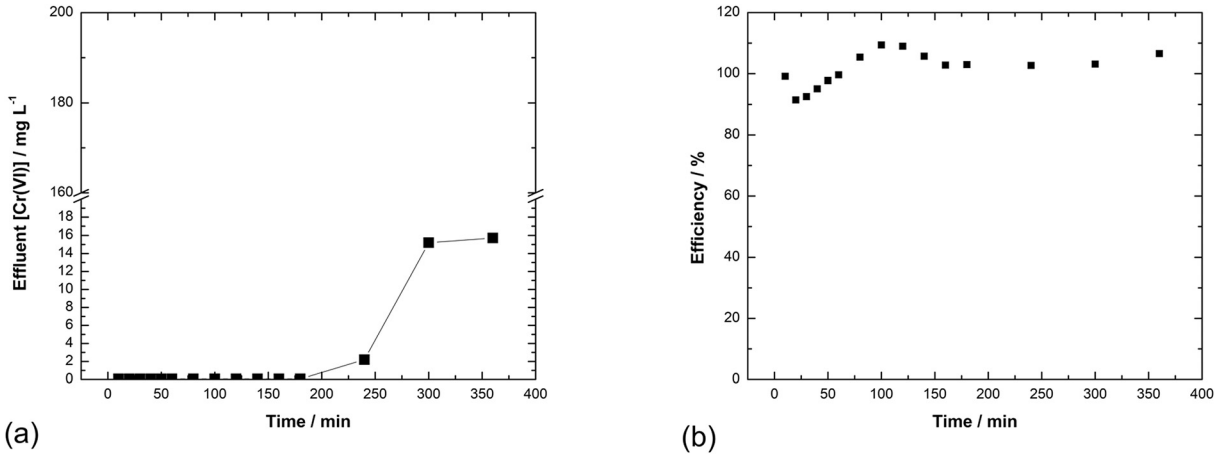

Fig. 7 Long term removal results with carbon anodes showing breakthrough of Cr(VI) into the cell effluent after 6 hours of operation. (a) Effluent [Cr(VI)] *versus* time and (b) charge efficiency of the process. Applied potential was 1.5 V with a 200 ppm Cr(VI) feed solution at pH 1.5 and flow rate of 12 ml min^{-1}.

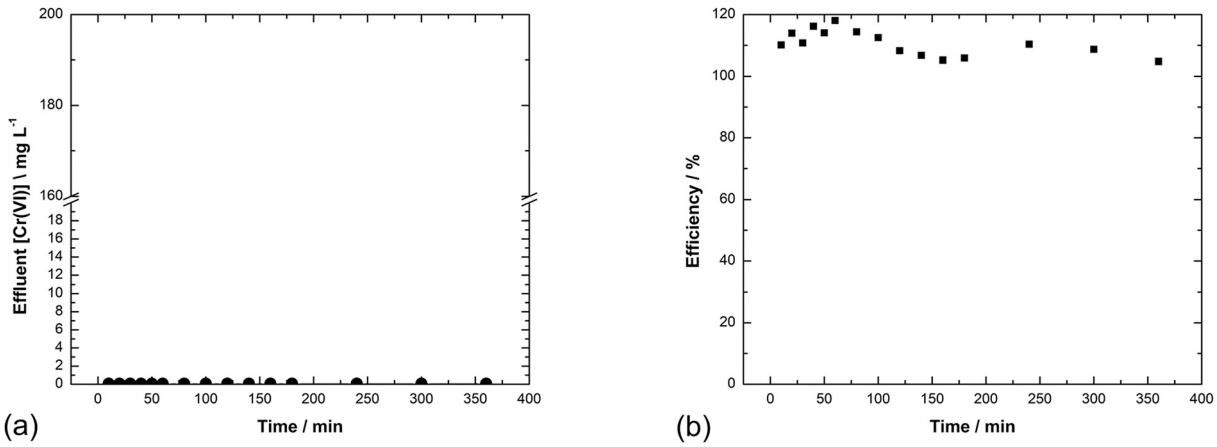

Fig. 8 Long term removal results with mixed-metal oxide showing complete reduction of Cr(VI) for six hours of operation. (a) Effluent [Cr(VI)] *versus* time and (b) charge efficiency of the process. Applied potential was 1.5 V with a 200 ppm Cr(VI) feed solution at pH 1.5 and flow rate of 12 ml min^{-1}.

Another observation born out in both the long-term tests and the varied pH/potential studies is the high charge efficiency of the reductions. In all of the studies, current data was collected and used to calculate the charge passed over the course of an experiment. These values were then compared to the theoretical minimum charge required to perform the reduction based on measurements of remaining [Cr(VI)]. In nearly all cases, the values exceed 100% efficiency and were never less than 91%, which has been seen previously in other all-carbon electrochemical separation systems in capacitive deionization.[29,30] During the long-term experiments, the charge passed was found for each period between samples in order to track efficiency changes. While there is variability in charge efficiency, it is consistently high, even when the carbon-based cell begins to allow unconverted Cr(VI) in the effluent. Some of this can be explained by the near-spontaneous character of the reduction reaction in the presence of the carbon anodes, as a control experiment at pH 1.5 with no applied potential did show a 4% reduction in Cr(VI) concentration. Additional spontaneous reduction under applied potential could also be due to further infiltration of the carbon film anodes by Cr(VI) where locally acidic conditions would be present and oxidation of additional carbon by Cr(VI) could take place. What is clearly demonstrated, however, is the overwhelming majority of the current input to the cell is used to drive the reduction of hexavalent chromium.

After these experiments were completed, the carbon cell was disassembled, and the individual anodes were tested to determine their resistivity. It was hypothesized that if oxidation or other electrochemically-based damage had occurred to the anodes, that their resistivity would be higher than an unused piece of the same material. Two pieces of each carbon anode from the long-term reduction experiment and samples from an unused carbon anode were cut into rectangles. Due to the small size of the anodes, only 2 pieces

could be produced from each electrode. The leads of a multimeter were placed in the center of a strip of anode 3.5 cm from one another, and the resistance value was read from the multimeter. Based on the cross-sectional area of the pieces and the 3.5 cm path length, resistivity values were calculated for each piece. A complete table of values is given in Table S2. Resistance measurements showed that there was a marked increase in resistivity for all 3 anodes compared to an unused specimen: up to 2980 Ω cm in the cell *versus* 26.92 Ω cm in fresh material. Additionally, the "bottom" two electrodes in the cell were substantially more resistive than the "top" electrode, with resistivities of 929.2 Ω cm at the bottom, 2980 Ω cm in the center, and 36.72 Ω cm at the top. Increased resistivity is consistent with oxidation of the carbon and with the loss of chromium reduction seen in the long-term experiment.[24,27,31] The uneven oxidation across the cell "height" could be a result of inconsistent flow through the cell caused by slight differences in compression and cell assembly. Cyclic voltammograms were also carried out at 10 mV s^{-1} in 0.1 M H_2SO_4 to determine changes in the capacitance of the electrodes. Dramatic loss of area in these curves was seen for the LiCAP carbon film anodes after the long-term separation, correlating with the increases in resistance that were measured (Fig. S25). While these measurements were undertaken on a single cell after a long-term test and were not the focus of this work, identifying the underlying causes of these differences in electrode utilization is an area of interest for future studies.

While the present study has focused on Cr(VI), there exist many metals that need to be separated from industrial waste streams such as Ag, Cu, and Ni, among many others. The ability to remove these metals using an electrically-driven process would be advantageous. Similar concepts to those shown in this work could be used for these other metals with plating occurring on a carbon cathode and discharge occurring capacitively at the anode and faradaic at the cathode. The ease of the process combined with the possibility of metal recovery would be useful.

Commercial system sizing estimates

Multiple factors need to be taken into account when determining the commercial viability for an electrochemical water treatment process. Before addressing cost implications, the ability for the system to reasonably meet the removal goals at an industrial site needs to be addressed. Waste byproduct from industrial processes such as electropolishing or metal finishing applications can generate hundreds of milligrams per liter of hexavalent chromium that must be removed from the wastewater prior to discharge to the local municipality. Flow rates can span a wide range, but 5–50 gallons per minute can be considered as practical wastewater flow rates. Using the charge efficiencies generated in the small-scale separation studies, which were at or above 100%, projections can be made for the current needed to fit flow rates for more practical industrial systems. Using 1–5 gallons per minute as example flow rates for an individual electrochemical cell, the current required can be plotted as a function of the influent Cr(VI) concentration (Fig. 9). At 5 gallons per minute and an influent [Cr(VI)] of 200 ppm, just over 350 A is required for full reduction to Cr(III) to take place. Assuming one electrochemical cell could handle that amperage, only 10 electrochemical cells would be required to handle a full 50 gallons per minute. In future work, the lifetime of the electrode materials and materials of construction will be taken into account. Direct cost comparisons will also be carried out to incumbent SMBS chemical reduction processes.

Conclusions

This work demonstrates that proper cell design can overcome mass transport limitations and allow a heterogeneous reaction to process hexavalent chromium water down to ppb levels in a representative commercial waste stream. With a residence time of <60 seconds, this process is in line with existing commercial solutions for wastewater processing. Further implantation will require a demonstration of economic viability when implemented at scale.

Due to the low potential requirement (≤1.5 V) and high charge efficiency, the power requirement would be low for such a system, only 450 W for a 300 A system. With electricity being the only feedstock required to carry out the reaction, the operational expenses will otherwise be minimal. To displace the incumbent process, sulfite reduction *via* SMBS, the capital costs will likely need to be brought down to a low enough value to result in a <3 year return on investment (ROI) with a <1 year ROI being particularly desirable. Lower cost carbon electrodes could enable this quicker ROI, but future work will need to extend the lifetime of these carbon anodes by either optimizing cycling time, increasing carbon

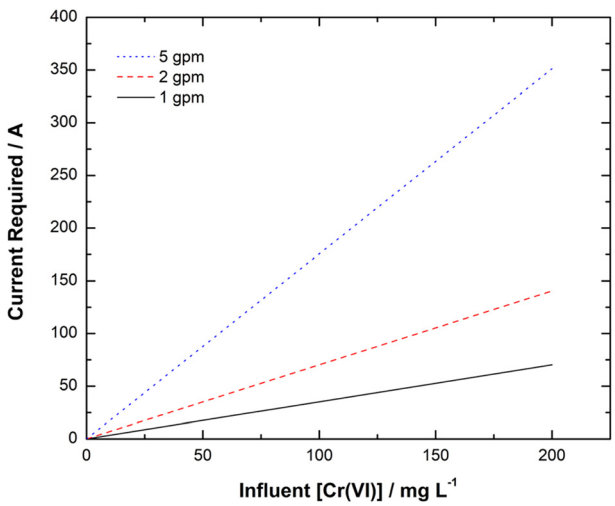

Fig. 9 Current required to reduce Cr(VI) to Cr(III) as a function of both concentration and flow rate.

loading, or decreasing the rate of carbon oxidation while maximizing the capacitive capability of the carbon.

Author contributions

J. L., A. R., C. L. and, C. D. designed experiments. C. D. prepared solutions and electrochemical cells. C. D. ran separation studies. J. L. and A. R. conducted potentiostat studies. J. L. and C. L. conducted scale up analysis. J. L., A. R., and C. D. analyzed data and wrote the manuscript.

Conflicts of interest

C. D., A. R., C. L., and J. L. have financial interest in PowerTech Water, Inc. d/b/a ElectraMet. There are no other conflicts of interest to report.

Data availability

The data supporting this article have been included as part of the supplementary information (SI).

Supplementary information is available. See DOI: https://doi.org/10.1039/d5ew00828j.

Acknowledgements

T. Smith at LiCAP Technologies for characterization information on the carbon anode films used in this work. J. Rentschler for aid in experimental design.

References

1 K. E. Ukhurebor, U. O. Aigbe, R. B. Onyancha, W. Nwankwo, O. A. Osibote, H. K. Paumo, O. M. Ama, C. O. Adetunji and I. U. Siloko, Effect of hexavalent chromium on the environment and removal techniques: A review, *J. Environ. Manage.*, 2021, **280**, 111809, DOI: 10.1016/j.jenvman.2020.111809.

2 R. Saha, R. Nandi and B. Saha, Sources and toxicity of hexavalent chromium, *J. Coord. Chem.*, 2011, **64**(10), 1782–1806, DOI: 10.1080/00958972.2011.583646.

3 C. Pellerin and S. M. Booker, Reflections on hexavalent chromium: health hazards of an industrial heavyweight, *Environ. Health Perspect.*, 2000, **108**(9), A402–A407, DOI: 10.1289/ehp.108-a402.

4 J. E. McLean, L. S. McNeill, M. A. Edwards and J. L. Parks, Hexavalent chromium review, part 1: Health effects, regulations, and analysis, *J. AWWA*, 2012, **104**(6), E348–E357, DOI: 10.5942/jawwa.2012.104.0091.

5 B. Xie, C. Shan, Z. Xu, X. Li, X. Zhang, J. Chen and B. Pan, One-step removal of Cr(VI) at alkaline pH by UV/sulfite process: Reduction to Cr(III) and in situ Cr(III) precipitation, *Chem. Eng. J.*, 2017, **308**, 791–797, DOI: 10.1016/j.cej.2016.09.123.

6 C. Su and R. D. Ludwig, Treatment of Hexavalent Chromium in Chromite Ore Processing Solid Waste Using a Mixed Reductant Solution of Ferrous Sulfate and Sodium Dithionite, *Environ. Sci. Technol.*, 2005, **39**(16), 6208–6216, DOI: 10.1021/es050185f.

7 L. Legrand, A. El Figuigui, F. Mercier and A. Chausse, Reduction of Aqueous Chromate by Fe(II)/Fe(III) Carbonate Green Rust: Kinetic and Mechanistic Studies, *Environ. Sci. Technol.*, 2004, **38**(17), 4587–4595, DOI: 10.1021/es035447x.

8 S. Hao, Y. Feng, D. Wang, J. Cho, C. Qiu, T.-U. Wi, Z. Xu, Z. Yu, C. Sellers and S. Zou, *et al.*, Electrochemical Removal of Se(IV) from Wastewater Using RuO2-Based Catalysts, *Nano Lett.*, 2025, **25**(6), 2547–2553, DOI: 10.1021/acs.nanolett.4c06344.

9 R. Chen, T. Sheehan, J. L. Ng, M. Brucks and X. Su, Capacitive deionization and electrosorption for heavy metal removal, *Environ. Sci.: Water Res. Technol.*, 2020, **6**(2), 258–282, DOI: 10.1039/C9EW00945K.

10 A. D. Sapp, H. Tian and M. Z. Bazant, Deionization shock waves and ionic separations in heterogeneous porous media, *Phys. Rev. Fluids*, 2024, **9**(7), 073701, DOI: 10.1103/PhysRevFluids.9.073701.

11 S. Aralekallu, M. Palanna, S. Hadimani, C. P. K. Prabhu, V. A. Sajjan, M. O. Thotiyl and L. K. Sannegowda, Biologically inspired catalyst for electrochemical reduction of hazardous hexavalent chromium, *Dalton Trans.*, 2020, **49**(42), 15061–15071, DOI: 10.1039/D0DT02752A.

12 A. K. Golder, A. K. Chanda, A. N. Samanta and S. Ray, Removal of hexavalent chromium by electrochemical reduction–precipitation: Investigation of process performance and reaction stoichiometry, *Sep. Purif. Technol.*, 2011, **76**(3), 345–350, DOI: 10.1016/j.seppur.2010.11.002.

13 S. Srinivas and A. Senthil Kumar, High-Performance Electrocatalytic Reduction and Sensing of Hazardous Hexavalent Chromium Using a Redox-Active Binol Species-Impregnated Carbon Nanofiber-Modified Electrode, *J. Phys. Chem. C*, 2022, **126**(19), 8296–8311, DOI: 10.1021/acs.jpcc.2c00317.

14 F. Rodriguez-Valadez, C. Ortiz-Éxiga, J. G. Ibanez, A. Alatorre-Ordaz and S. Gutierrez-Granados, Electroreduction of Cr(VI) to Cr(III) on Reticulated Vitreous Carbon Electrodes in a Parallel-Plate Reactor with Recirculation, *Environ. Sci. Technol.*, 2005, **39**(6), 1875–1879, DOI: 10.1021/es049091g.

15 E. P. L. Roberts and H. Yu, Chromium removal using a porous carbon felt cathode, *J. Appl. Electrochem.*, 2002, **32**(10), 1091–1099, DOI: 10.1023/A:1021282015050.

16 C. M. Stern, D. W. Hayes, L. O. Kgoadi and N. Elgrishi, Emerging investigator series: carbon electrodes are effective for the detection and reduction of hexavalent chromium in water, *Environ. Sci.: Water Res. Technol.*, 2020, **6**(5), 1256–1261, DOI: 10.1039/D0EW00146E.

17 X. Su, A. Kushima, C. Halliday, J. Zhou, J. Li and T. A. Hatton, Electrochemically-mediated selective capture of heavy metal chromium and arsenic oxyanions from water, *Nat. Commun.*, 2018, **9**(1), 4701, DOI: 10.1038/s41467-018-07159-0.

18 M. E. Suss, S. Porada, X. Sun, P. M. Biesheuvel, J. Yoon and V. Presser, Water desalination via capacitive deionization: what is it and what can we expect from it?, *Energy Environ. Sci.*, 2015, **8**(8), 2296–2319, DOI: 10.1039/C5EE00519A.

19 T.-H. Chen, Y.-A. Chen, S.-W. Tsai, D.-M. Wang and C.-H. Hou, Development of an integrated capacitive-electrodialysis process (CapED) for continuous, low-energy electrochemical deionization, *Sep. Purif. Technol.*, 2021, **274**, 119063, DOI: 10.1016/j.seppur.2021.119063.

20 B. Avasarala, R. Moore and P. Haldar, Surface oxidation of carbon supports due to potential cycling under PEM fuel cell conditions, *Electrochim. Acta*, 2010, **55**(16), 4765–4771, DOI: 10.1016/j.electacta.2010.03.056.

21 C. Zhang, D. He, J. Ma, W. Tang and T. D. Waite, Faradaic reactions in capacitive deionization (CDI) - problems and possibilities: A review, *Water Res.*, 2018, **128**, 314–330, DOI: 10.1016/j.watres.2017.10.024.

22 X. Gao, A. Omosebi, J. Landon and K. Liu, Surface charge enhanced carbon electrodes for stable and efficient capacitive deionization using inverted adsorption–desorption behavior, *Energy Environ. Sci.*, 2015, **8**(3), 897–909, DOI: 10.1039/C4EE03172E.

23 X. Gao, A. Omosebi, J. Landon and K. Liu, Dependence of the Capacitive Deionization Performance on Potential of Zero Charge Shifting of Carbon Xerogel Electrodes during Long-Term Operation, *J. Electrochem. Soc.*, 2014, **161**(12), E159, DOI: 10.1149/2.0561412jes.

24 D. Deng, B. Chen, C. Zhao, M. A. Anderson and Y. Wang, Importance of Anode/Cathode Mass Loadings on Capacitive Deionization Performance, *J. Electrochem. Soc.*, 2021, **168**(5), 053503, DOI: 10.1149/1945-7111/ac00f8.

25 M. Pourbaix, *Atlas of Electrochemical Equilibria in Aqueous Solutions*, Pergamon Press, Oxford, New York, 1966.

26 G. T. K. K. Gunasooriya and J. K. Nørskov, Analysis of Acid-Stable and Active Oxides for the Oxygen Evolution Reaction, *ACS Energy Lett.*, 2020, **5**(12), 3778–3787, DOI: 10.1021/acsenergylett.0c02030.

27 N. E. Holubowitch, A. Omosebi, X. Gao, J. Landon and K. Liu, Membrane-free electrochemical deoxygenation of aqueous solutions using symmetric activated carbon electrodes in flow-through cells, *Electrochim. Acta*, 2019, **297**, 163–172, DOI: 10.1016/j.electacta.2018.11.106.

28 X. Gao, S. Porada, A. Omosebi, K. L. Liu, P. M. Biesheuvel and J. Landon, Complementary surface charge for enhanced capacitive deionization, *Water Res.*, 2016, **92**, 275–282, DOI: 10.1016/j.watres.2016.01.048.

29 A. Omosebi, X. Gao, J. Rentschler, J. Landon and K. Liu, Continuous operation of membrane capacitive deionization cells assembled with dissimilar potential of zero charge electrode pairs, *J. Colloid Interface Sci.*, 2015, **446**, 345–351, DOI: 10.1016/j.jcis.2014.11.013.

30 A. Omosebi, X. Gao, N. Holubowitch, Z. Li, J. Landon and K. Liu, Anion Exchange Membrane Capacitive Deionization Cells, *J. Electrochem. Soc.*, 2017, **164**(9), E242, DOI: 10.1149/2.0461709jes.

31 X. Gao, A. Omosebi, J. Landon and K. Liu, Voltage-Based Stabilization of Microporous Carbon Electrodes for Inverted Capacitive Deionization, *J. Phys. Chem. C*, 2018, **122**(2), 1158–1168, DOI: 10.1021/acs.jpcc.7b08968.